

Measurement of the Branching Fraction $\mathcal{B}(\Lambda_c^+ \rightarrow pK^-\pi^+)$

A. Zupanc,²² C. Bartel,²⁴ N. Gabyshev,⁴ I. Adachi,¹³ H. Aihara,⁶¹ D. M. Asner,⁴⁷ V. Aulchenko,⁴ T. Aushev,²¹ A. M. Bakich,⁵⁵ A. Bala,⁴⁸ K. Belous,¹⁹ B. Bhuyan,¹⁵ A. Bondar,⁴ G. Bonvicini,⁶⁷ A. Bozek,⁴² M. Bračko,^{33,22} T. E. Browder,¹² D. Červenkov,⁵ M.-C. Chang,⁸ V. Chekelian,³⁴ B. G. Cheon,¹¹ K. Chilikin,²¹ R. Chistov,²¹ I.-S. Cho,⁶⁹ K. Cho,²⁶ V. Chobanova,³⁴ S.-K. Choi,¹⁰ Y. Choi,⁵⁴ D. Cinabro,⁶⁷ J. Dalseno,^{34,57} M. Danilov,^{21,36} Z. Doležal,⁵ Z. Drásal,⁵ D. Dutta,¹⁵ K. Dutta,¹⁵ S. Eidelman,⁴ D. Epifanov,⁶¹ H. Farhat,⁶⁷ J. E. Fast,⁴⁷ M. Feindt,²⁴ T. Ferber,⁷ V. Gaur,⁵⁶ S. Ganguly,⁶⁷ A. Garmash,⁴ R. Gillard,⁶⁷ R. Glattauer,¹⁸ Y. M. Goh,¹¹ B. Golob,^{31,22} J. Haba,¹³ K. Hayasaka,³⁸ H. Hayashii,³⁹ X. H. He,⁴⁹ Y. Hoshi,⁵⁹ W.-S. Hou,⁴¹ M. Huschle,²⁴ H. J. Hyun,²⁹ T. Iijima,^{38,37} A. Ishikawa,⁶⁰ R. Itoh,¹³ Y. Iwasaki,¹³ T. Iwashita,²⁵ I. Jaegle,¹² T. Julius,³⁵ J. H. Kang,⁶⁹ E. Kato,⁶⁰ Y. Kato,³⁷ T. Kawasaki,⁴⁴ H. Kichimi,¹³ D. Y. Kim,⁵³ H. J. Kim,²⁹ J. B. Kim,²⁷ J. H. Kim,²⁶ M. J. Kim,²⁹ Y. J. Kim,²⁶ K. Kinoshita,⁶ J. Klucar,²² B. R. Ko,²⁷ P. Kodyš,⁵ S. Korpar,^{33,22} P. Križan,^{31,22} P. Krokovny,⁴ B. Kronenbitter,²⁴ T. Kuhr,²⁴ T. Kumita,⁶³ A. Kuzmin,⁴ Y.-J. Kwon,⁶⁹ S.-H. Lee,²⁷ J. Li,⁵² Y. Li,⁶⁶ J. Libby,¹⁶ C. Liu,⁵¹ Y. Liu,⁶ Z. Q. Liu,¹⁷ D. Liventsev,¹³ J. MacNaughton,¹³ K. Miyabayashi,³⁹ H. Miyata,⁴⁴ R. Mizuk,^{21,36} G. B. Mohanty,⁵⁶ A. Moll,^{34,57} R. Mussa,²⁰ E. Nakano,⁴⁶ M. Nakao,¹³ H. Nakazawa,⁷⁰ Z. Natkaniec,⁴² M. Nayak,¹⁶ E. Nedelkovska,³⁴ M. Niiyama,²⁸ N. K. Nisar,⁵⁶ S. Nishida,¹³ O. Nitoh,⁶⁴ S. Ogawa,⁵⁸ S. L. Olsen,⁵² W. Ostrowicz,⁴² P. Pakhlov,^{21,36} G. Pakhlova,²¹ C. W. Park,⁵⁴ H. Park,²⁹ H. K. Park,²⁹ T. K. Pedlar,³² R. Pestotnik,²² M. Petrič,²² L. E. Piilonen,⁶⁶ M. Ritter,³⁴ M. Röhrken,²⁴ A. Rostomyan,⁷ S. Ryu,⁵² H. Sahoo,¹² T. Saito,⁶⁰ Y. Sakai,¹³ S. Sandilya,⁵⁶ L. Santelj,²² T. Sanuki,⁶⁰ V. Savinov,⁵⁰ O. Schneider,³⁰ G. Schnell,^{1,14} C. Schwanda,¹⁸ D. Semmler,⁹ K. Senyo,⁶⁸ O. Seon,³⁷ M. E. Sevir,³⁵ M. Shapkin,¹⁹ C. P. Shen,² T.-A. Shibata,⁶² J.-G. Shiu,⁴¹ B. Shwartz,⁴ A. Sibidanov,⁵⁵ F. Simon,^{34,57} Y.-S. Sohn,⁶⁹ A. Sokolov,¹⁹ E. Solovieva,²¹ S. Stanič,⁴⁵ M. Starič,²² M. Steder,⁷ T. Sumiyoshi,⁶³ U. Tamponi,^{20,65} K. Tanida,⁵² G. Tatishvili,⁴⁷ Y. Teramoto,⁴⁶ K. Trabelsi,¹³ M. Uchida,⁶² S. Uehara,¹³ Y. Unno,¹¹ S. Uno,¹³ P. Urquijo,³ Y. Usov,⁴ C. Van Hulse,¹ P. Vanhoefer,³⁴ G. Varner,¹² K. E. Varvell,⁵⁵ A. Vinokurova,⁴ V. Vorobyev,⁴ M. N. Wagner,⁹ C. H. Wang,⁴⁰ P. Wang,¹⁷ X. L. Wang,⁶⁶ M. Watanabe,⁴⁴ Y. Watanabe,²³ K. M. Williams,⁶⁶ E. Won,²⁷ H. Yamamoto,⁶⁰ Y. Yamashita,⁴³ S. Yashchenko,⁷ Y. Yook,⁶⁹ Z. P. Zhang,⁵¹ V. Zhilich,⁴ and V. Zhulanov⁴

(Belle Collaboration)

¹University of the Basque Country UPV/EHU, 48080 Bilbao

²Beihang University, Beijing 100191

³University of Bonn, 53115 Bonn

⁴Budker Institute of Nuclear Physics SB RAS and Novosibirsk State University, Novosibirsk 630090

⁵Faculty of Mathematics and Physics, Charles University, 121 16 Prague

⁶University of Cincinnati, Cincinnati, Ohio 45221

⁷Deutsches Elektronen-Synchrotron, 22607 Hamburg

⁸Department of Physics, Fu Jen Catholic University, Taipei 24205

⁹Justus-Liebig-Universität Gießen, 35392 Gießen

¹⁰Gyeongsang National University, Chinju 660-701

¹¹Hanyang University, Seoul 133-791

¹²University of Hawaii, Honolulu, Hawaii 96822

¹³High Energy Accelerator Research Organization (KEK), Tsukuba 305-0801

¹⁴IKERBASQUE, Basque Foundation for Science, 48011 Bilbao

¹⁵Indian Institute of Technology Guwahati, Assam 781039

¹⁶Indian Institute of Technology Madras, Chennai 600036

¹⁷Institute of High Energy Physics, Chinese Academy of Sciences, Beijing 100049

¹⁸Institute of High Energy Physics, Vienna 1050

¹⁹Institute for High Energy Physics, Protvino 142281

²⁰INFN-Sezione di Torino, 10125 Torino

²¹Institute for Theoretical and Experimental Physics, Moscow 117218

²²J. Stefan Institute, 1000 Ljubljana

²³Kanagawa University, Yokohama 221-8686

²⁴Institut für Experimentelle Kernphysik, Karlsruher Institut für Technologie, 76131 Karlsruhe

²⁵Kavli Institute for the Physics and Mathematics of the Universe (WPI), University of Tokyo, Kashiwa 277-8583

²⁶Korea Institute of Science and Technology Information, Daejeon 305-806

²⁷Korea University, Seoul 136-713

- ²⁸Kyoto University, Kyoto 606-8502
²⁹Kyungpook National University, Daegu 702-701
³⁰École Polytechnique Fédérale de Lausanne (EPFL), Lausanne 1015
³¹Faculty of Mathematics and Physics, University of Ljubljana, 1000 Ljubljana
³²Luther College, Decorah, Iowa 52101
³³University of Maribor, 2000 Maribor
³⁴Max-Planck-Institut für Physik, 80805 München
³⁵School of Physics, University of Melbourne, Victoria 3010
³⁶Moscow Physical Engineering Institute, Moscow 115409
³⁷Graduate School of Science, Nagoya University, Nagoya 464-8602
³⁸Kobayashi-Maskawa Institute, Nagoya University, Nagoya 464-8602
³⁹Nara Women's University, Nara 630-8506
⁴⁰National United University, Miao Li 36003
⁴¹Department of Physics, National Taiwan University, Taipei 10617
⁴²H. Niewodniczanski Institute of Nuclear Physics, Krakow 31-342
⁴³Nippon Dental University, Niigata 951-8580
⁴⁴Niigata University, Niigata 950-2181
⁴⁵University of Nova Gorica, 5000 Nova Gorica
⁴⁶Osaka City University, Osaka 558-8585
⁴⁷Pacific Northwest National Laboratory, Richland, Washington 99352
⁴⁸Panjab University, Chandigarh 160014
⁴⁹Peking University, Beijing 100871
⁵⁰University of Pittsburgh, Pittsburgh, Pennsylvania 15260
⁵¹University of Science and Technology of China, Hefei 230026
⁵²Seoul National University, Seoul 151-742
⁵³Soongsil University, Seoul 156-743
⁵⁴Sungkyunkwan University, Suwon 440-746
⁵⁵School of Physics, University of Sydney, New South Wales 2006
⁵⁶Tata Institute of Fundamental Research, Mumbai 400005
⁵⁷Excellence Cluster Universe, Technische Universität München, 85748 Garching
⁵⁸Toho University, Funabashi 274-8510
⁵⁹Tohoku Gakuin University, Tagajo 985-8537
⁶⁰Tohoku University, Sendai 980-8578
⁶¹Department of Physics, University of Tokyo, Tokyo 113-0033
⁶²Tokyo Institute of Technology, Tokyo 152-8550
⁶³Tokyo Metropolitan University, Tokyo 192-0397
⁶⁴Tokyo University of Agriculture and Technology, Tokyo 184-8588
⁶⁵University of Torino, 10124 Torino
⁶⁶CNP, Virginia Polytechnic Institute and State University, Blacksburg, Virginia 24061
⁶⁷Wayne State University, Detroit, Michigan 48202
⁶⁸Yamagata University, Yamagata 990-8560
⁶⁹Yonsei University, Seoul 120-749
⁷⁰National Central University, Chung-li 32054

(Received 30 December 2013; revised manuscript received 5 May 2014; published 25 July 2014)

We present the first model-independent measurement of the absolute branching fraction of the $\Lambda_c^+ \rightarrow pK^-\pi^+$ decay using a data sample of 978 fb^{-1} collected with the Belle detector at the KEKB asymmetric-energy e^+e^- collider. The number of Λ_c^+ baryons is determined by reconstructing the recoiling $D^{(*)-}\bar{p}\pi^+$ system in events of the type $e^+e^- \rightarrow D^{(*)-}\bar{p}\pi^+\Lambda_c^+$. The branching fraction is measured to be $\mathcal{B}(\Lambda_c^+ \rightarrow pK^-\pi^+) = (6.84 \pm 0.24_{-0.27}^{+0.21})\%$, where the first and second uncertainties are statistical and systematic, respectively.

DOI: 10.1103/PhysRevLett.113.042002

PACS numbers: 14.20.Lq, 13.30.Eg, 13.66.Bc

The hadronic decay $\Lambda_c^+ \rightarrow pK^-\pi^+$ is the reference mode for the measurements of branching fractions of the Λ_c^+ baryon to any other final state [1]. In addition, this is the most common decay mode in studies where a Λ_c^+ baryon is included in the final state of the decay chain, such as the

exclusive and inclusive decay rate measurements of b -flavored mesons and baryons or the measurements of fragmentation fractions of charm and bottom quarks. The Particle Data Group combines several measurements from the ARGUS and CLEO Collaborations [2–8] to

determine $\mathcal{B}(\Lambda_c^+ \rightarrow pK^-\pi^+) = (5.0 \pm 1.3)\%$, where the dominant contribution to the quoted uncertainty originates from the model dependence of the branching fraction extraction [9]. A precise measurement of the branching fraction $\mathcal{B}(\Lambda_c^+ \rightarrow pK^-\pi^+)$ can, therefore, significantly improve the precision of branching fractions of other Λ_c^+ decays and, also, those of decays of b -flavored mesons and baryons involving Λ_c^+ .

In this Letter, we present the first model-independent measurement of the absolute branching fraction of $\Lambda_c^+ \rightarrow pK^-\pi^+$ decays [10] that improves the precision of previous model-dependent measurements by a factor of 5. We use a data sample, corresponding to an integrated luminosity of 978 fb^{-1} , collected at or near the $\Upsilon(nS)$ ($n = 1, 2, 3, 4, 5$) resonances with the Belle detector at the KEKB asymmetric-energy e^+e^- collider.

The absolute branching fraction of the $\Lambda_c^+ \rightarrow pK^-\pi^+$ decay is given by

$$\mathcal{B}(\Lambda_c^+ \rightarrow pK^-\pi^+) = \frac{N(\Lambda_c^+ \rightarrow pK^-\pi^+)}{N_{\text{inc}}^{\Lambda_c} f_{\text{bias}} \epsilon(\Lambda_c^+ \rightarrow pK^-\pi^+)}, \quad (1)$$

where $N_{\text{inc}}^{\Lambda_c}$ is the number of inclusively reconstructed Λ_c^+ baryons, $N(\Lambda_c^+ \rightarrow pK^-\pi^+)$ is the number of reconstructed $\Lambda_c^+ \rightarrow pK^-\pi^+$ decays within the inclusive Λ_c^+ sample, $\epsilon(\Lambda_c^+ \rightarrow pK^-\pi^+)$ is the reconstruction efficiency of $\Lambda_c^+ \rightarrow pK^-\pi^+$ decays within the inclusive Λ_c^+ sample, and the factor f_{bias} takes into account potential dependence of the inclusive Λ_c^+ reconstruction efficiency on the Λ_c^+ decay mode.

The $e^+e^- \rightarrow c\bar{c}$ events that contain Λ_c^+ baryons produced through the reactions $e^+e^- \rightarrow c\bar{c} \rightarrow D^{(*)-} \bar{p}\pi^+\Lambda_c^+$ are fully reconstructed in two steps. In the first, no requirements are placed on the daughters of the Λ_c^+ baryons in order to obtain an inclusive sample of Λ_c^+ events that is used as the denominator in the calculation of the branching fraction. The number of inclusively reconstructed Λ_c^+ baryons is extracted from the distribution of events in the missing mass recoiling against the $D^{(*)-} \bar{p}\pi^+$ system,

$M_{\text{miss}}(D^{(*)} p\pi) = \sqrt{p_{\text{miss}}^2(D^{(*)} p\pi)}$, where $p_{\text{miss}}(D^{(*)} p\pi) = p_{e^+} + p_{e^-} - p_{D^{(*)}} - p_p - p_\pi$ is the missing four-momentum in the event. Here, p_{e^+} and p_{e^-} are the known four-momenta of the colliding positron and electron beams, respectively, and $p_{D^{(*)}}$, p_p , and p_π are the measured four-momenta of the reconstructed $D^{(*)}$, the antiproton, and the pion, respectively. Correctly reconstructed events produce a peak in the $M_{\text{miss}}(D^{(*)} p\pi)$ distribution at the nominal Λ_c^+ mass. In the second step, we search for the decay products of the $\Lambda_c^+ \rightarrow pK^-\pi^+$ decay within the inclusive Λ_c^+ sample reconstructed in the first step. In particular, we require that there be only three charged tracks, consistent with being a kaon, pion, and proton, in the rest of the event.

The Belle detector is a large-solid-angle magnetic spectrometer that consists of a silicon vertex detector

(SVD), a 50-layer central drift chamber (CDC), an array of aerogel threshold Cherenkov counters (ACC), a barrel-like arrangement of time-of-flight scintillation counters (TOF), and an electromagnetic calorimeter (ECL) comprised of CsI(Tl) crystals located inside a superconducting solenoid coil that provides a 1.5 T magnetic field. An iron flux-return located outside of the coil is instrumented to detect K_L^0 mesons and to identify muons. The detector is described in detail elsewhere [11,12]. We use Monte Carlo (MC) events generated with EVTGEN [13] and JETSET [14] and, then, processed through the detailed detector simulation implemented in GEANT3 [15]. Final state radiation from charged particles is simulated during event generation using the PHOTOS package [16]. The simulated samples for e^+e^- annihilation to $q\bar{q}$ ($q = u, d, s, c$, and b) are equivalent to six times the integrated luminosity of the data and are used to develop methods to separate signal events from backgrounds, identify types of background events, determine the reconstruction efficiency, and parametrize the distributions needed for the extraction of the signal decays.

Charged particles are reconstructed with the CDC and the SVD. Each is required to have an impact parameter with respect to the interaction point (IP) of less than 1.5 cm along the positron beam direction and less than 0.5 cm in the plane transverse to the positron beam direction. A likelihood ratio for a given track to be a kaon, pion, or proton is obtained by utilizing energy-loss measurements in the CDC, light yield measurements from the ACC, and time-of-flight information from the TOF. Photons are detected with the ECL and are required to have energies in the laboratory frame of at least 50 (100) MeV in the ECL barrel (end caps). Neutral pion candidates are reconstructed using photon pairs with an invariant mass between 120 and 150 MeV/ c^2 , which corresponds to $\pm 3.2\sigma$ around the nominal π^0 mass [1], where σ represents the resolution. Neutral kaon candidates are reconstructed using pairs of oppositely charged pions with an invariant mass within $\pm 20 \text{ MeV}/c^2$ ($\pm 5\sigma$) of the nominal K^0 mass.

We reconstruct the charmed pseudoscalar mesons in the following twelve decay modes: $D^0 \rightarrow K^-\pi^+$, $K^-\pi^+\pi^0$, $K^-\pi^+\pi^+\pi^-$, $K^-\pi^+\pi^+\pi^-\pi^0$, $K_S^0\pi^+\pi^-$, or $K_S^0\pi^+\pi^-\pi^0$; $D^+ \rightarrow K^-\pi^+\pi^+$, $K^-\pi^+\pi^+\pi^0$, $K_S^0\pi^+$, $K_S^0\pi^+\pi^0$, $K_S^0\pi^+\pi^+\pi^-$, or $K^+K^-\pi^+$. In order to reject background from $e^+e^- \rightarrow B\bar{B}$ events and combinatorial background, the D momentum in the e^+e^- frame is required to be greater than 2.3 to 2.5 GeV/ c , depending on the decay mode. To further increase the purity of the reconstructed sample of charmed pseudoscalar mesons, we combine several variables into a single output variable using the NeuroBayes neural network [17]: the distance between the decay and the production vertices of the D candidate in the transverse plane, where the D production vertex is defined by the intersection of its trajectory with the IP region, the χ^2 of the vertex fit of the D candidate, the cosine of the angle between the D momentum and the vector joining its decay

and production vertices in the transverse plane; for two-body $D \rightarrow K\pi$ decays, the cosine of the angle between the kaon momentum and the boost direction of the laboratory frame in the D rest frame, the particle identification likelihood ratios of charged tracks in the final state, and, for the D decay modes with a π^0 , the smaller of the two daughter photons' energies. The cut on the network output variable is optimized for each D decay mode individually by maximizing $S/\sqrt{S+B}$, where S (B) refers to the signal (background) yield in the signal region that is defined as the $\pm 3\sigma$ interval around the nominal D meson mass, where σ is the decay-mode-dependent invariant-mass resolution and ranges from 4 to 12 MeV/c^2 . After optimization, the D purity within the signal region increases from 17% to 42% while only around 16% of signal D candidates are lost. We use only the D candidates in the signal region in the remainder of the analysis. More details about the D selection procedure are given in Ref. [18]. Neutral (charged) D mesons are combined with a charged (neutral) pion candidate to form charged D^* candidates. We keep only D^* candidates in the $\pm 3\sigma$ region around the nominal value of the mass difference $m(D^*) - m(D)$.

The D and D^* candidates are combined with a proton or antiproton and remaining charged pion candidates to form $D^{(*)}p\pi$ combinations that represent a sample of inclusively reconstructed charm baryons. A kinematic fit to each $D^{(*)}p\pi$ candidate is performed in which the particles are required to originate from a common point inside the IP region and the D mass is constrained to the nominal value [1]. We divide the reconstructed charm baryons into the right sign (RS) $D^{(*)-}\bar{p}\pi^+$, wrong sign (WS) $D^{(*)-}p\pi^-$, and $D^{(*)+}\bar{p}\pi^-$ charge combinations based on the charm quantum number and baryon number of the $D^{(*)}p\pi$ combinations relative to their total electric charge. The WS sample, by definition, cannot contain correctly reconstructed Λ_c^+ candidates, so it is used to study properties of the background. We retain inclusively reconstructed Λ_c^+ candidates with $2.0 \text{ GeV}/c^2 < M_{\text{miss}}(D^{(*)}p\pi) < 2.5 \text{ GeV}/c^2$. In 15% of the events, we find more than one $D^{(*)}p\pi$ candidate; in such cases we select at random a single RS (WS) candidate for further analysis, if only RS (WS) candidates are found, or a single RS and a single WS candidate, if RS and WS candidates are found in an event.

Figure 1 shows the distributions of $M_{\text{miss}}(D^{(*)}p\pi)$ for RS and WS candidates. A prominent peak at the nominal Λ_c^+ mass is visible in the spectrum of the RS sample, while the spectrum of the WS sample is featureless. The yield of inclusively reconstructed Λ_c^+ baryons is determined by performing a binned maximum likelihood fit to the $M_{\text{miss}}(D^{(*)}p\pi)$ distribution of RS candidates. The inclusively reconstructed Λ_c^+ candidates fall into three categories: correctly reconstructed $D^{(*)}p\pi$ combinations from signal events (signal), correctly reconstructed $D^{(*)}p\pi$ candidates from $e^+e^- \rightarrow D^{(*)-}\bar{p}\pi^+\Lambda_c^+X$ events, where X represents one or two additional particles produced in the process of

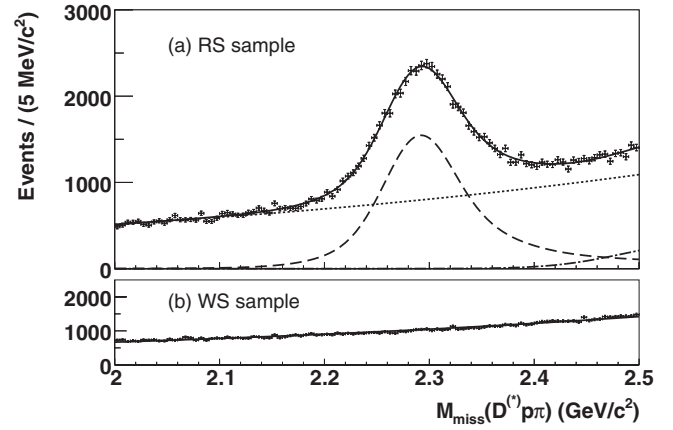


FIG. 1. The $M_{\text{miss}}(D^{(*)}p\pi)$ data distributions (points with error bars) for inclusively reconstructed Λ_c^+ baryons from the (a) RS and (b) WS samples with superimposed fit results (solid line). The contributions of signal, combinatorial and missing X background are shown with the dashed, dotted, and dashed-dotted lines, respectively.

hadronization that are missed in the reconstruction (missing X background), and all other combinations (combinatorial background), which also contribute to the WS sample.

The signal candidates are parametrized as the sum of two components, a core and an upper-tail part, to describe the contribution of events with an undetected initial state radiation (ISR) photon [19]. The core (upper-tail) component of the signal is described with the sum of two (one) Gaussian functions (function) and a bifurcated Gaussian function. In the fit, we fix all parameters, including the fraction of ISR events, to the values determined from the MC sample except for the means and the common resolution scaling factor of the first and the second Gaussian function. The missing X background is parametrized as the sum of two Gaussian functions, the first for the case of one missing particle, and the second for the case of two missing particles. All the fit parameters except the normalization are fixed. We use an exponential function to describe the combinatorial background, where the single shape parameter is fixed to the value determined by the fit to the $M_{\text{miss}}(D^{(*)}p\pi)$ distribution in the WS sample [20]. The results of the fits for the WS and RS samples are shown in Fig. 1. The number of inclusively reconstructed Λ_c^+ baryons is found to be $N_{\text{incl}}^{\Lambda_c^+} = 36447 \pm 432$, where the uncertainty is statistical only.

After reconstructing the inclusive sample of Λ_c^+ baryons, we proceed with the reconstruction of $\Lambda_c^+ \rightarrow pK^-\pi^+$ decays within the inclusive Λ_c^+ sample. This is performed by requiring exactly three charged tracks to be present in the rest of the event with a net total charge equal to the charge of the inclusively reconstructed Λ_c^+ candidate. The track whose charge is opposite that of the inclusive Λ_c^+ candidate is assigned to be the kaon. From the two same-sign tracks, we identify the proton based on the particle identification likelihood ratios; the remaining track is assumed to

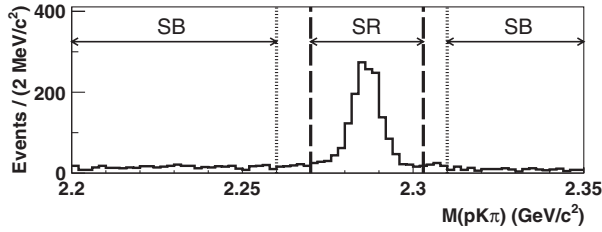


FIG. 2. The $M(pK\pi)$ distribution of exclusively reconstructed $\Lambda_c^+ \rightarrow pK^-\pi^+$ candidates within the inclusive Λ_c^+ sample. The dashed (dotted) vertical lines indicate the borders of signal regions (SR) and sideband regions (SB).

be a pion. Figure 2 shows the invariant-mass distribution of exclusively reconstructed $\Lambda_c^+ \rightarrow pK^-\pi^+$ decays within the inclusive Λ_c^+ sample. A clear peak at the nominal mass of the Λ_c^+ can be seen above a very low background.

MC studies show that the Λ_c^+ inclusive reconstruction efficiency depends weakly on the Λ_c^+ decay mode, and therefore, the inclusively reconstructed Λ_c^+ sample does not represent a truly inclusive sample of Λ_c^+ baryons. This effect is described with the factor $f_{\text{bias}} = \epsilon_{\Lambda_c^+ \rightarrow f}^{\text{inc}} / \bar{\epsilon}_{\Lambda_c^+}^{\text{inc}}$ in Eq. (1) and is given by the ratio of Λ_c^+ inclusive reconstruction efficiency for $\Lambda_c^+ \rightarrow f$ decays, $\epsilon_{\Lambda_c^+ \rightarrow f}^{\text{inc}}$, and the average Λ_c^+ inclusive reconstruction efficiency, $\bar{\epsilon}_{\Lambda_c^+}^{\text{inc}} = \sum_i \mathcal{B}(\Lambda_c^+ \rightarrow i) \epsilon_{\Lambda_c^+ \rightarrow i}^{\text{inc}}$. In the case of $f = pK^-\pi^+$, the f_{bias} value determined by MC simulation that includes all known Λ_c^+ decays is found to be consistent with unity and the product of the tag bias and the exclusive reconstruction efficiency is $f_{\text{bias}} \epsilon(\Lambda_c^+ \rightarrow pK^-\pi^+) = (54.5 \pm 0.6)\%$, where the uncertainty is due to the limited MC statistics.

The number of exclusively reconstructed $\Lambda_c^+ \rightarrow pK^-\pi^+$ decays within the inclusive Λ_c^+ sample is determined by performing a fit to the $M_{\text{miss}}(D^{(*)}p\pi)$ distribution of candidates within the signal regions (SR) and sideband regions (SB) of $M(pK\pi)$. The main reason to perform a fit to the $M_{\text{miss}}(D^{(*)}p\pi)$ distribution rather than the $M(pK\pi)$ distribution is that, in the former case, the systematic uncertainty related to the parametrization of $M_{\text{miss}}(D^{(*)}p\pi)$ distributions cancels to a large extent in the ratio of exclusively and inclusively reconstructed Λ_c^+ candidates [see Eq. (1)] while, in the latter case, it does not. The fits to the $M_{\text{miss}}(D^{(*)}p\pi)$ distributions of candidates within the signal and sideband regions of $M(pK\pi)$ are performed in the same way and using the same parametrization as the fit to the $M_{\text{miss}}(D^{(*)}p\pi)$ distribution of all inclusive Λ_c^+ candidates. We first fit candidates in the WS sample to determine the shape parameter of the combinatorial background that we then fix in the fit of the RS sample. In the RS fit, the signal shape parameters are fixed to the values found in the fit to the total inclusive Λ_c^+ sample. Figure 3 shows the results of the fits to the RS and WS $M_{\text{miss}}(D^{(*)}p\pi)$ distributions of exclusively reconstructed Λ_c^+ candidates within the signal and sideband regions of $M(pK\pi)$. The signal yields are found to be

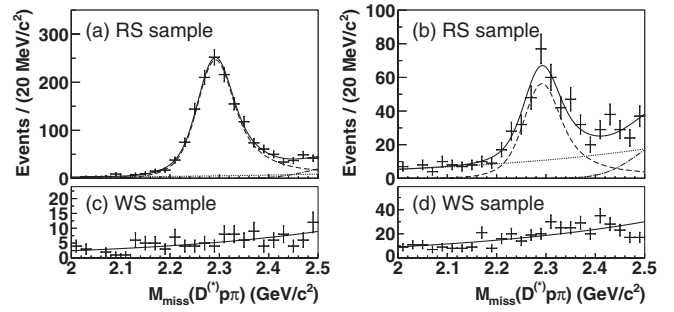


FIG. 3. The $M_{\text{miss}}(D^{(*)}p\pi)$ data distributions (points with error bars) of exclusively reconstructed $\Lambda_c^+ \rightarrow pK^-\pi^+$ candidates. (a) and (c) for the SR region and (b) and (d) SB region of $M(pK\pi)$ for the RS and WS samples, respectively, with superimposed fit results (solid line). The contributions of signal, combinatorial and missing X background are shown with the dashed, dotted, and dashed-dotted lines, respectively.

$N_{\text{excl}}^{\text{SR}} = 1457 \pm 44$ and $N_{\text{excl}}^{\text{SB}} = 332 \pm 27$, where the uncertainties are statistical.

The number of exclusively reconstructed $\Lambda_c^+ \rightarrow pK^-\pi^+$ decays within the inclusive Λ_c^+ sample (where both exclusive and inclusive Λ_c^+ candidates are correctly reconstructed) is given by $N(\Lambda_c^+ \rightarrow pK^-\pi^+) = N_{\text{excl}}^{\text{SR}} - r_{\text{SR}}^{\text{SB}} N_{\text{excl}}^{\text{SB}}$, where $N_{\text{excl}}^{\text{SR(SB)}}$ is the yield of correctly reconstructed inclusive Λ_c^+ candidates from the fit to the $M_{\text{miss}}(D^{(*)}p\pi)$ distribution of candidates within the signal (sideband) region of the $M(pK\pi)$ distribution. The ratio $r_{\text{SR}}^{\text{SB}}$ is formed from the yields of correctly reconstructed inclusive Λ_c^+ candidates but wrongly reconstructed exclusive Λ_c^+ candidates within the signal and sideband regions. These candidates peak in $M_{\text{miss}}(D^{(*)}p\pi)$ but not in $M(pK\pi)$. The ratio is determined on a simulated sample of events to be $r_{\text{SR}}^{\text{SB}} = 0.296 \pm 0.015$. The number of exclusively reconstructed $\Lambda_c^+ \rightarrow pK^-\pi^+$ decays is, thus, $N(\Lambda_c^+ \rightarrow pK^-\pi^+) = 1359 \pm 45$, where the uncertainty includes the $N_{\text{excl}}^{\text{SR}}$ and $N_{\text{excl}}^{\text{SB}}$ statistical uncertainties. The branching fraction, given by Eq. (1), is $\mathcal{B}(\Lambda_c^+ \rightarrow pK^-\pi^+) = (6.84 \pm 0.24)\%$, where the uncertainty includes both exclusive [$N(\Lambda_c^+ \rightarrow pK^-\pi^+)$] and inclusive ($N_{\text{incl}}^{\Lambda_c^+}$) uncertainties.

As a check, we extract the branching fractions of $\Lambda_c^+ \rightarrow pK^-\pi^+$ decays for each $D^{(*)+}$ decay mode individually; these are found to be in good agreement with each other as well as with the nominal result. As mentioned above, the alternative way to determine the number of exclusively reconstructed $\Lambda_c^+ \rightarrow pK^-\pi^+$ decays is to perform a fit to the $M(pK\pi)$ distribution: we find 1208 ± 41 correctly reconstructed $\Lambda_c^+ \rightarrow pK^-\pi^+$ decays within the $2.16 \text{ GeV}/c^2 < M_{\text{miss}}(D^{(*)}p\pi) < 2.38 \text{ GeV}/c^2$ region and the resulting branching fraction, $(6.78 \pm 0.24)\%$, in excellent agreement with the nominal result. We perform another model-independent measurement of $\mathcal{B}(\Lambda_c^+ \rightarrow pK^-\pi^+)$ in events of $e^+e^- \rightarrow D^{(*)-} \bar{p}\pi^+ \Lambda_c^+$ and $e^+e^- \rightarrow \bar{D}^0 \bar{p}\Lambda_c^+$ that utilizes a cut-based $D^{(*)}$ selection. Here, we determine the number of

TABLE I. Summary of systematic uncertainties.

Source	Uncertainty (%)
Tracking	1.1
Proton identification	0.4
Efficiency	1.1
Dalitz model	1.1
f_{bias}	1.5
Background subtraction	+0.5 -0.9
Fit model	+1.7 -2.9
Total	+3.0 -3.9

$\Lambda_c^+ \rightarrow pK^-\pi^+$ decays within the inclusive Λ_c^+ sample by a fit to the missing energy of the event, which is expected to be zero for correctly reconstructed signal events. The measured branching fraction, $(7.04 \pm 0.38)\%$, where the uncertainty is statistical, is found to be in good agreement with the nominal result.

Systematic uncertainties in the calculation of the branching fraction arise due to imperfect knowledge of the efficiency of the exclusive reconstruction of $\Lambda_c^+ \rightarrow pK^-\pi^+$ decays within the inclusive Λ_c^+ sample and the modeling of signal and background contributions in fits to the $M_{\text{miss}}(D^{(*)}p\pi)$ distributions of inclusive and exclusive candidates. Since the branching fraction is determined relative to the number of inclusively reconstructed Λ_c^+ baryons, the systematic uncertainties in the reconstruction of the $D^{(*)}p\pi$ system cancel. The estimated systematic uncertainties are summarized in Table I and described below. The systematic uncertainty due to charged-track reconstruction efficiency is estimated to be 0.35% per track (1.1% in total) from partially reconstructed $D^{*+} \rightarrow D^0(K_S^0\pi^+\pi^-)\pi^+$ decays. We estimate the uncertainty due to proton identification (0.4%) using a $\Lambda \rightarrow p\pi^-$ sample. The systematic uncertainty due to the requirement that there are no additional tracks present in an event after the exclusive reconstruction of $\Lambda_c^+ \rightarrow pK^-\pi^+$ candidates within the inclusive Λ_c^+ sample is estimated as follows. We compare the ratios of events with a correctly reconstructed exclusive Λ_c^+ candidate within the inclusive Λ_c^+ sample with and without any additional tracks detected as determined on simulated and data samples. We find the ratios to be small and in good agreement and, therefore, assign no additional systematic uncertainty. We include, as a source of systematic uncertainty, the statistical uncertainty of the MC-determined efficiency (1.1%). The reconstruction efficiency of $\Lambda_c^+ \rightarrow pK^-\pi^+$ decays is found to vary weakly across the $pK^-\pi^+$ Dalitz distribution. In calculating $\mathcal{B}(\Lambda_c^+ \rightarrow pK^-\pi^+)$, we use the Dalitz-plot-integrated MC efficiency. The decay amplitude in the MC simulation is the incoherent sum of all known resonant two-body contributions. We vary the relative contributions of these intermediate states within their uncertainties [1] to

estimate the systematic uncertainty due to the Dalitz model to be 1.1%. Possible differences in relative rates of individual Λ_c^+ decay modes between MC simulation and data that impact the $f_{\text{bias}}\epsilon(\Lambda_c^+ \rightarrow pK^-\pi^+)$ determination are estimated by studying the distributions of the number of charged particles and neutral pions produced in Λ_c^+ decays in MC simulation and data [18]; the corresponding systematic uncertainty is estimated to be 1.5%. We propagate the statistical uncertainty of the $r_{\text{SR}}^{\text{SB}}$ ratio and perform the background subtraction using the upper and lower $M(Kp\pi)$ sidebands only and take the difference from the nominal value to estimate the systematic uncertainty due to background subtraction (in total $^{+0.5}_{-0.9}\%$). We estimate the systematic uncertainty due to the $M_{\text{miss}}(D^{(*)}p\pi)$ fit model by varying the shape parameter of the combinatorial background within its uncertainties (as obtained from the WS sample fit) ($\pm 0.7\%$), using a second-order polynomial to describe combinatorial background instead of the exponential function ($^{+1.5}_{-2.8}\%$), using a parametrization for the one- or two-missing-particle backgrounds separately instead of the nominal mixture of the two ($\pm 0.07\%$), giving an additional contribution to the total fit function that describes a possible peaking contribution from $e^+e^- \rightarrow D^{(*)-}\bar{p}\pi^+\Sigma_c(2455/2520)$ events ($\pm 0.01\%$), varying the signal shape parameters obtained from the fit to the inclusive sample in fits to the signal and sideband regions of the $M(pK\pi)$ distribution ($\pm 0.3\%$), and varying the fraction of ISR within the signal model by $\pm 20\%$, which is the precision of the prediction given in Ref. [19] ($\pm 0.3\%$). The total systematic uncertainty is the sum of the above contributions in quadrature.

In summary, we perform the first model-independent measurement of the absolute branching fraction of the decay $\Lambda_c^+ \rightarrow pK^-\pi^+$ using the Belle final data sample corresponding to 978 fb^{-1} . We measure $\mathcal{B}(\Lambda_c^+ \rightarrow pK^-\pi^+) = [6.84 \pm 0.24(\text{stat})^{+0.21}_{-0.27}(\text{syst})]\%$, which represents a fivefold improvement in precision over previous model-dependent determinations. This measurement will also improve significantly the precision of the branching fraction of other Λ_c^+ decays and of decays of b -flavored mesons and baryons involving Λ_c^+ .

We thank the KEKB group for excellent operation of the accelerator, the KEK cryogenics group for efficient solenoid operations, and the KEK computer group, the NII, and PNNL/EMSL for valuable computing and SINET4 network support. We acknowledge support from MEXT, JSPS, and Nagoya's TLPRC (Japan); ARC and DIISR (Australia); FWF (Austria); NSFC (China); MSMT (Czechia); CZF, DFG, and VS (Germany); DST (India); INFN (Italy); MOE, MSIP, NRF, GSDC of KISTI, BK21Plus, and WCU (Korea); MNiSW and NCN (Poland); MES and RFAAE (Russia); ARRS (Slovenia); IKERBASQUE and UPV/EHU (Spain); SNSF (Switzerland); NSC and MOE (Taiwan); and DOE and NSF (U.S.).

- [1] J. Beringer *et al.* (Particle Data Group), *Phys. Rev. D* **86**, 010001 (2012).
- [2] H. Albrecht *et al.* (ARGUS Collaboration), *Phys. Lett. B* **207**, 109 (1988).
- [3] G. D. Crawford *et al.* (CLEO Collaboration), *Phys. Rev. D* **45**, 752 (1992).
- [4] H. Albrecht *et al.* (ARGUS Collaboration), *Z. Phys. C* **56**, 1 (1992).
- [5] H. Albrecht *et al.* (ARGUS Collaboration), *Phys. Lett. B* **269**, 234 (1991).
- [6] T. Bergfeld *et al.* (CLEO Collaboration), *Phys. Lett. B* **323**, 219 (1994).
- [7] H. Albrecht *et al.* (ARGUS Collaboration), *Phys. Rep.* **276**, 224 (1996).
- [8] P. Avery *et al.* (CLEO Collaboration), *Phys. Rev. D* **43**, 3599 (1991).
- [9] For a review of the model-dependent measurements, see “ Λ_c^+ branching fractions” on page 1386 in Ref. [1].
- [10] Throughout this Letter, charge-conjugate modes are included.
- [11] J. Brodzicka *et al.* (Belle Collaboration), *Prog. Theor. Exp. Phys.* **2012**, 4D001 (2012).
- [12] A. Abashian *et al.* (Belle Collaboration), *Nucl. Instrum. Methods Phys. Res., Sect. A* **479**, 117 (2002).
- [13] D. Lange, *Nucl. Instrum. Methods Phys. Res., Sect. A* **462**, 152 (2001).
- [14] T. Sjöstrand, *Comput. Phys. Commun.* **82**, 74 (1994).
- [15] R. Brun, F. Bruyant, M. Maire, A. McPherson, and P. Zancarini, CERN Report No. CERN-DD-EE-84-1, 1987.
- [16] E. Barberio and Z. Was, *Comput. Phys. Commun.* **79**, 291 (1994).
- [17] M. Feindt and U. Kerzel, *Nucl. Instrum. Methods Phys. Res., Sect. A* **559**, 190 (2006).
- [18] A. Zupanc *et al.* (Belle Collaboration), *J. High Energy Phys.* **09** (2013) 139.
- [19] M. Benayoun, S. Eidelman, V. Ivanchenko, and Z. Silagadze, *Mod. Phys. Lett. A* **14**, 2605 (1999).
- [20] The MC simulation shows that the WS sample correctly models the combinatorial background in the RS sample.